A PROOF-OF-PRINCIPLE POWER CONVERTER FOR THE SPALLATION NEUTRON SOURCE RF SYSTEM*

W.A. Reass#, J.D. Doss, M.G. Fresquez, D.A. Miera, J.S. Mirabal, P.J. Tallerico
Los Alamos National Laboratory,
P.O. Box 1663, MS H-827, Los Alamos, NM 87545

Abstract

The power converter for the SNS RF system is a fast pulsed power supply that transforms 7 kV, 3-phase ac input power into 120 kV pulses with an amplitude of 80 A, a flat-top pulse length of 1.1 ms, and a repetition rate of 60 Hz. The power converter accomplishes this transformation by rectifying the input power to 8 kV dc. This is followed by a high-frequency (20 kHz) switched mode dc-to-dc converter that has rise and fall times below 0.1 ms. (The required peak power for a pair of 2.5 MW/805 MHz klystrons is almost 10 MW, and the average power is 750 kW). Since the peak and average power requirements are a significant advance of the state-of-the art for switched-mode power supplies, it is prudent to design and build a scale version of the circuit. This proof-of-principle version of the circuit is a 1/100th voltage model that operates with an input of 100 V and produces an output of 1200 V. The critical components of the converter are the IGBT switches and the high voltage transformer. The design of the low-power converter involved a novel high voltage transformer and the same switches that will be used in the high power converter. Simulations have been performed and data that shows agreement between the computer simulation and the scale model will be presented.

1 INTRODUCTION

The simplified block diagram of the (full-scale) IGBT converter-modulator is shown in Figure 1. This system topology offers a number of engineering advantages as compared to other long pulse modulator designs. The converter-modulator derives it's plus and minus buss voltages from a standard substation open frame cast-core transformer. The transformers and the associated support and personnel safety equipment is placed along the length of the LINAC, as placement requires, in utility sheds. This semi-remote equipment is "dumb"; it does not require control I/O or monitoring equipment. A utility umbilical cable connects to the converter-modulator assembly and the AC feed is locally switched and rectified in a utility cabinet, part of the converter-modulator assembly. A step-start network is required to minimize turn-on transients from the resonance of the capacitor bank, substation transformer leakage, and line harmonic filter networks. The rectifier stacks provide a buss voltage of + 4 kV and – 4 kV. The energy storage networks utilize self-clearing metalized hazy polypropylene capacitors. With these capacitors, soft degradation can be monitored and capacitors can be replaced during a normal maintenance cycle, if needed. Switching is provided by a series string of 8 IGBT's for each plus and minus rail (for each phase). For three phase switching, 48 devices (3 x 16) are required. We have chosen 1700 volt devices because their superior switch current ratings and significantly lower (switching) loss as compared to higher voltage devices. With our chosen snubber networks, and relatively low string voltage, IGBT timing skews of 250 nS can easily be tolerated and yet maintain transient voltages within device ratings. A unique boost-transformer has been designed for the polyphase voltage step-up at 20 kHz. This transformer, whose core configuration is shown in Figure 2 is called a polyphase "Y". This transformer core design helps to provide a low leakage inductance, good balance between phases (core flux paths are all equal to one another), and minimal cost. Special magnetic alloys are expensive; this design uses half the core material as compared to 3 individual "C" cores. Transformer secondary shunt-peaking is desirable to tune out leakage inductance and maximize output voltage. Various shunt-peaking capacitor types may be used, but mica is a good low loss dielectric system for this voltage and frequency. Rectification is provided by series strings of ion-implanted diodes with 1400 volt, 75 Amp, and ~50 nS reverse recovery ratings. The output filter network is optimized to adequately filter the 120 kHz rectification pulses, yet have little stored energy. At the end of each klystron video pulse, the stored energy must be dissipated, in addition, in a klystron arc-down condition, excessive stored energy would be detrimental to the klystron. In series with each klystron, dI/dT limiting networks reduce the rate of energy deposition to help ensure continued klystron reliability.

2 COMPUTER MODELING

The system design topology has been thoroughly scrutinized with computer modeling to determine system performance, component sensitivities, circuit efficiency, and fault tolerance. Due to the repetitive pulse loading of the utility grid, line harmonic and power factor issues are a concern. Fortunately, a simple circuit with power factor correction capacitors and line filter chokes can provide almost unity power factor and line harmonics that are within IEEE specifications at full power operation.
Unfortunately, the resulting line impedance resonates with the transformer leakage inductance and capacitor filter network during start-up, resulting in over-voltage of the

0-7803-5573-3/99/$10.00@1999 IEEE.

capacitor bank. This problem can be alleviated by the use of a resistive step-start system. The step-start system must be cycled during any brownout or interruption of utility service, i.e. from a lighting strike or other anomaly. IGBT performance can be more reliably assured by the choice of appropriate snubber networks to help equalize dynamic voltage division. With our chosen parameters, the snubber loss for each IGBT is about 90 watts with ideal timing of the IGBT transistors. With a 250 nS timing skew, the peak transient voltage across the IGBT reaches about 1450 volts, well within the devices 1700 volt ratings, as shown in Figure 3. Continuous operation with this timing skew (250 nS) results in about 180 watts being dissipated in the snubber network resistor. The transformer design for this system also requires careful consideration. Transformer magnetizing and leakage inductance play a critical role in system performance. Fortunately, some leeway is provided by the use of shunt-peaking capacitors in the transformer secondary. The effect on the klystron output voltage, with steps of shunt-peaking capacitance, is shown in Figure 4. This results in changes of IGBT switch current. High values of shunt-peaking capacitance over-compensate the circuit and reduce voltage output and increase IGBT switching current. The circuit model is run with the IGBT's operating with a full 180-degree conduction angle. In the actual system operation, pulse width modulation will be utilized to regulate and flattop the klystron cathode voltage pulse. A detail of the cathode voltage pulse with full 180-degree conduction is shown in Figure 5. At all times the cathode voltage is above the required 120 kV. A reduced conduction angle will provide the appropriate output voltage. In addition, other computer modeling has shown that the turn-on overshoot can be totally removed by reducing the conduction angle of the IGBT's first few pulses. A klystron cathode voltage waveform at reduced voltage, due to reduced IGBT conduction angle is shown in Figure 6. What is interesting about this result is that there is no increase in the apparent output ripple. (The output fundamental is still 120 kHz, but there are significantly higher Fourier frequency components, which the output filter network smoothes more effectively). A critical parameter for any klystron modulator system is the energy deposited in the klystron during a fault condition. Our IGBT configuration is a very benign system; the total fault energy deposited in a klystron is about 8 joules, only in the event the converter is not interrupted during its' 1.1ms switching cycle. This result is shown in Figure 7. In addition, the peak fault current in the klystron is less than 200 Amps, with low dI/dT's.

*Work funded by the US Department of Energy and operated by the University of California under contract W-7405-ENG-36

Email: wreass@lanl.gov

3 SCALE MODEL RESULTS:

The scale model converter worked as designed with results that compare well to the computer model, the first time it was turned on. In addition, some results required further computer analysis to help analyze what we observed. It was counter-intuitive to us that at reduced output voltage and conduction angle, output ripple would not increase. The full output voltage from the scale model converter is shown in Figure 8 and compares well with Figure 5. With reduced conduction angle, the output voltage is shown in Figure 9, and it also compares well with Figure 6. Fortunately, the most fun comes from analyzing and optimizing the system performance in our test set-up. We have been able to determine the effect on IGBT timing offsets and examine the resultant output ripple, which also has agreed with our computer analysis.

4 CONCLUSION:

The IGBT converter-modulator full-scale design is nearly complete. The concept and performance of the novel design topologies have been proven with the scale model version. Comparison with the computer predicted results furthers our resolution that this circuit topology will prove eminently successful. In addition, control electronic designs have been tested and evaluated that can directly operate our full power version. It is clear to us that this type of converter-modulator offers many significant advantages over other system designs and techniques. Among these advantages are that no crowbar system is required; a single point network I/O; a small inexpensive and dumb substation; and a low voltage energy store with self-clearing capacitors. Other advantages are the reliability of a completely solid-state system, minimal oil requirements, a small footprint less than competing designs, and safety advantages over H.V. anode modulation systems.

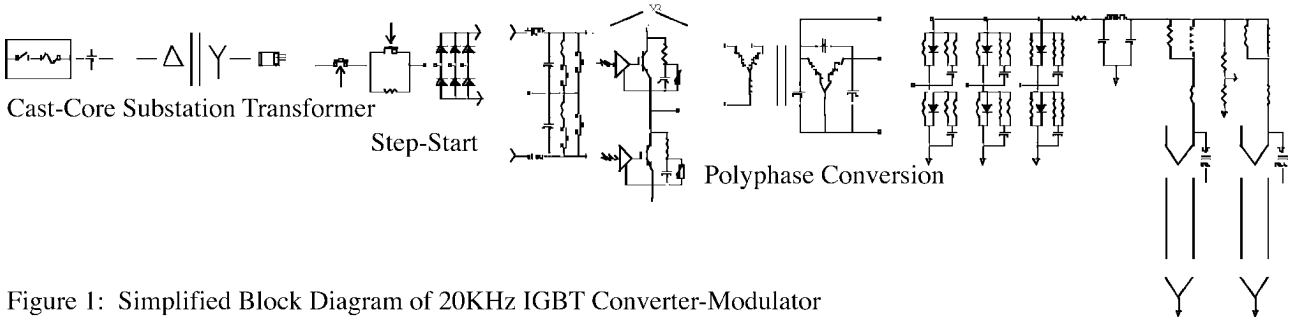

Figure 1: Simplified Block Diagram of 20KHz IGBT Converter-Modulator

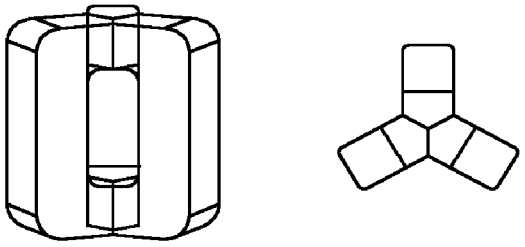

Figure 2: Polyphase Y Transformer

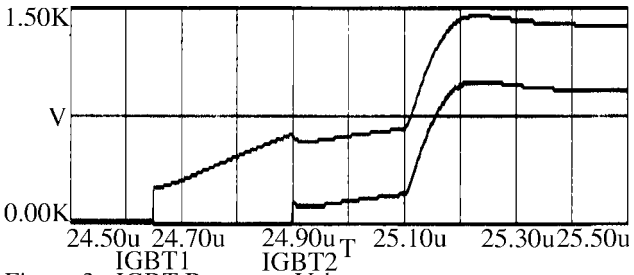

Figure 3: IGBT Recovery Voltage

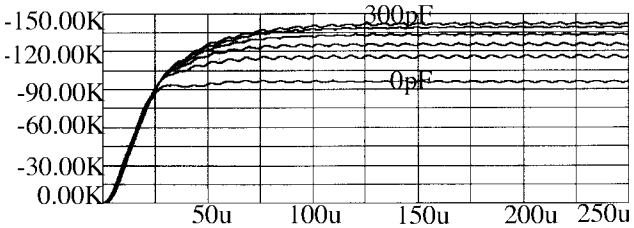

Figure 4: Cathode Voltage vs Peaking Capacitance

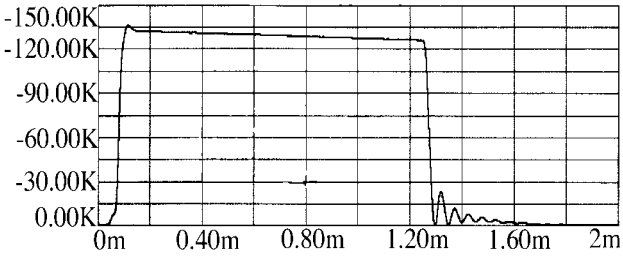

Figure 5: Computer Model Cathode Voltage

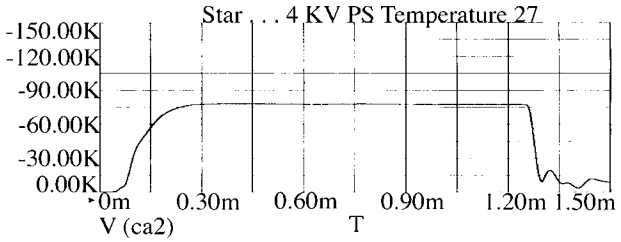

Figure 6: Computer Model at Reduced Output.

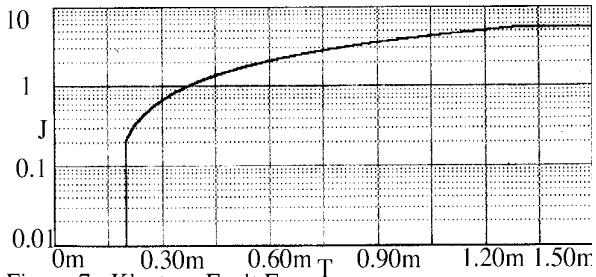

Figure 7: Klystron Fault Energy

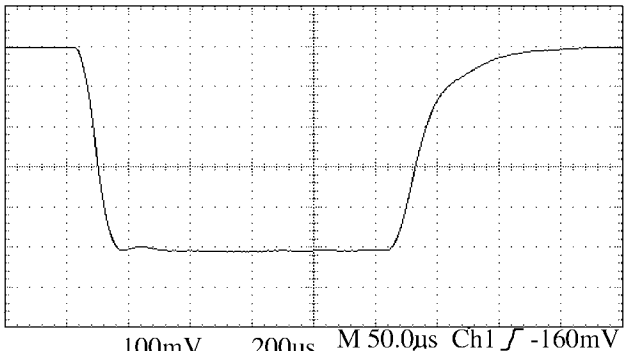

Figure 8: Scale Model Output Voltage

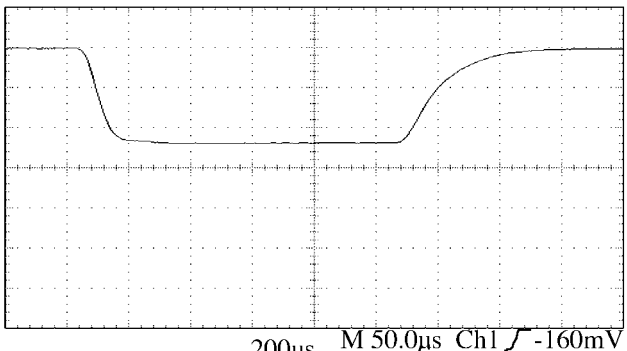

Figure 9: Scale Model at Reduced Output.